

Article

A Self-Disperse Copper-Based Catalyst Synthesized via a Dry Mixing Method for Acetylene Hydrochlorination

Yuru Fu ^{1,2}, Xi Sun ^{1,*}, Jian Zhang ¹ and Jiahui Huang ^{1,*}

¹ Dalian National Laboratory for Clean Energy, Dalian Institute of Chemical Physics, Chinese Academy of Sciences, Dalian 116023, China; fuyuru@dicp.ac.cn (Y.F.); jzhang1993@dicp.ac.cn (J.Z.)

² University of Chinese Academy of Sciences, Beijing 100049, China

* Correspondence: sunx27@dicp.ac.cn (X.S.); jiahuihuang@dicp.ac.cn (J.H.)

Abstract: Traditional methods for synthesizing single-site catalysts are typically complicated and require special chemicals due to their tendency to agglomerate. In this study, we present a self-disperse copper-based catalyst synthesized via a dry mixing method for acetylene hydrochlorination. During the reaction, the copper precursor compounds, i.e., CuBr, and CuI, were converted to CuCl. Subsequently, the formed CuCl crystals underwent a significant structural transformation, leading to the formation of small clusters and Cu single sites. The catalytic activity of 5% CuCl + C prepared through the dry mixing method decreased from 93.7% to 92.9% after 100 h of reaction under the condition of GHSV (C₂H₂) = 60 mL·h⁻¹·g⁻¹. A comparison of the 5% CuCl + C with the 5% CuCl/C obtained by the impregnation method reveals that the catalytic stability of the former was higher than the one prepared by the conventional impregnation method. The exceptional catalytic performance can be attributed to the reaction-induced active sites being highly dispersed and the porous structure of activated carbon being maximally preserved, which was confirmed by HAADF-STEM, BET, TPR, and TG. The reaction-induced dispersion of CuCl on carbon provides a new strategy for preparing single-site catalysts for acetylene hydrochlorination.

Keywords: acetylene hydrochlorination; dry mixing method; CuCl; single-site catalyst; reaction-induced dispersion



Citation: Fu, Y.; Sun, X.; Zhang, J.; Huang, J. A Self-Disperse Copper-Based Catalyst Synthesized via a Dry Mixing Method for Acetylene Hydrochlorination. *Catalysts* **2024**, *14*, 207. <https://doi.org/10.3390/catal14030207>

Academic Editors: Valeria La Parola and Leonarda Liotta

Received: 6 December 2023

Revised: 26 January 2024

Accepted: 26 January 2024

Published: 20 March 2024



Copyright: © 2024 by the authors. Licensee MDPI, Basel, Switzerland. This article is an open access article distributed under the terms and conditions of the Creative Commons Attribution (CC BY) license (<https://creativecommons.org/licenses/by/4.0/>).

1. Introduction

It has been recognized that single-site catalysts comprising isolated active centers [1–4] play significant roles in many industrially important chemical processes and have also attracted increasing research attention. The extremely high metal dispersity of a single-site catalyst meant that the metal is used sufficiently, providing an ideal strategy to produce cost-effective catalysts for commercializing supported metal catalysts, especially those required for precious metals [5–7].

The successful large-scale application of Au as a catalyst for the production of vinyl chloride monomer (VCM) via acetylene hydrochlorination that occurred in late 2015 is a landmark of gold catalysis, also highlighting the success of the single-site catalysis strategy [6]. As the main ingredient of PVC [8], about one-third of the approximately 50 million tons per year of worldwide VCM capacity is produced by acetylene hydrochlorination technology, which is mainly catalyzed by a supported HgCl₂ catalyst [5,9–11]. With the signing of the Minimata Convention, the mercury product will be phased-out compulsorily by 2022 due to it being extremely harmful to the environment and human beings [6,11–13]. As a result of Hutchings' pioneering work [14], which, in 1985, first predicted that gold would be the best catalyst for acetylene hydrochlorination, gold has replaced the extremely harmful mercury as a catalyst, with its successful commercialization announced by global chemicals company Johnson Matthey [6].

Although precious metals such as gold [3,7,15], platinum [16,17], and ruthenium [16,18–21] exhibit impressive performance for acetylene hydrochlorination, their high cost and large

carbon footprints make them less competitive and environmentally unfriendly. Copper, as a metal with abundant reserves on Earth, is highly appealing for use in the acetylene hydrochlorination reaction [11,20], but its activity and stability fall short of those of noble metals. In this case, researchers have attempted to improve the performance of copper-based catalysts by introducing modifiers either as dopants in the support [22–26] or co-deposited together with copper on the surface [11,20,27,28]. However, these methods often lead to complex preparation processes, increased production costs, reduced durability, and potential environmental contamination, as nitrogen–phosphorus compounds are used as modifiers.

In 1990, Yuchang Xie and his colleagues discovered that multiple salts and oxides can disperse spontaneously into monolayers on a carrier, which led to the development of a dry mixing method for material preparation [29]. This approach has broadened the preparation and application of catalysts. For example, Xie et al. heated a mixture of CuCl and a Na-zeolite at a suitable temperature, finding that the CuCl crystalline phase changed into a monolayer dispersion state on the surface of the zeolite, which had CO capacity and selectivity much higher than CO₂, CH₄, N₂, and H₂ for the separation of CO from gas mixtures containing CO₂. Xiao et al. found that a CuCl₂/HZSM-5 catalyst prepared using the dry mixing method exhibited much higher catalytic conversion in selective reduction of NO than a CuZSM-5 catalyst prepared using the ion-exchange method [30]. Wang et al. reported that the reaction-induced spreading of metal oxides was directly reflected in the catalytic properties of mixed metal oxide materials [31].

In this study, we used the dry mixing method with copper-based catalysts to solve the high cost and rapid deactivation of catalysts for acetylene hydrochlorination. The catalysts synthesized via the dry mixing method with relatively low metal content (5wt%) by mixing and grinding CuCl with a commercial activated carbon exhibited excellent stability in acetylene hydrochlorination. The dynamic catalyst evolution was uncovered by X-ray diffraction (XRD) and scanning transmission electron microscopy (STEM), suggesting the dispersion of CuCl crystals and the formation of small Cu clusters and single atoms, which allowed us to derive the correlation between the dispersion of CuCl crystals and the performance of catalysts.

2. Results and Discussion

2.1. The Change of CuX + C during Acetylene Hydrochlorination

CuX + C (X = Cl, Br, I), the mixture of activated carbon and CuX salts, was confirmed by SEM (see in Figure S1). A series of CuX + C (X = Cl, Br, I) was evaluated for acetylene hydrochlorination at 473 K and GHSV(C₂H₂) of 380 mL·h⁻¹·g⁻¹. The results, as shown in Figure 1a, indicated that CuX + C gradually showed catalytic activity and exhibited similar reaction tendencies, with the catalytic curves tending to converge under the induction of the reaction atmosphere. In Figure 1b, XRD detection was carried out on fresh and used 5% CuX + C (X = Cl, Br, I) catalysts to analyze the aggregation and dispersion state of Cu in the catalysts. X-ray diffraction (XRD) analysis revealed that diffraction peaks associated with CuI and CuBr in the CuI + C-u and CuBr + C-u disappeared. Furthermore, there were new diffraction peaks at 28.5°, 47.4°, and 56.3° in 5% CuBr + C-u and 5% CuI + C-u catalysts, which were the same as the CuCl peak position (JCPDS: 06–0344). Moreover, the intensity of the characteristic peak of the 5% CuCl + C catalyst diminished after the reaction relative to its intensity before the reaction. Combined with the observation that the conversion rate increased progressively with reaction time, these results suggest that copper compounds (CuI and CuBr) tended to transform into CuCl under reaction, which gradually dispersed or was consumed in the reaction atmosphere. The high concentration of chlorine in the reaction environment might be the reason for this, as well as the fact that CuCl has the lowest lattice energy compared to other copper compounds. This makes it easier for atoms to break out of the lattice bonding and disperse [31].

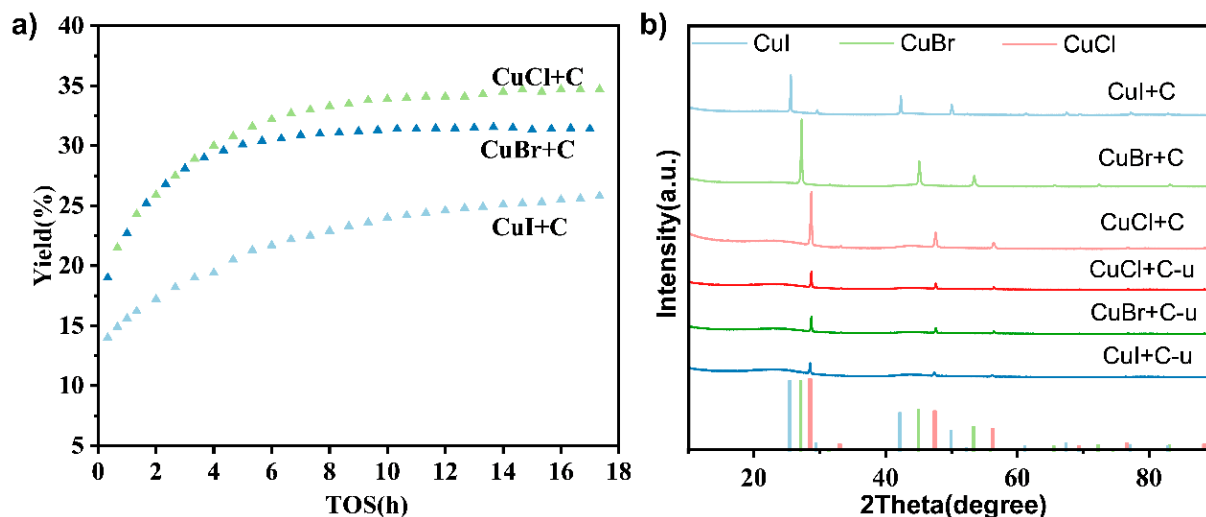


Figure 1. (a) The catalytic performance of a series of $\text{CuX} + \text{C}$ ($\text{X} = \text{Cl}, \text{Br}, \text{I}$). Test conditions: $\text{GHSV} (\text{C}_2\text{H}_2) = 380 \text{ mL}\cdot\text{h}^{-1}\cdot\text{g}^{-1}$, $V_{\text{HCl}}:V_{\text{C}_2\text{H}_2} = 1.1$, and $T = 180^\circ\text{C}$. (b) XRD patterns of the fresh and used Cu-based catalysts. $\text{CuX} + \text{C-u}$ represents used $\text{CuX} + \text{C}$.

2.2. The Reaction-Induced Dispersion of CuCl on Activated Carbon

To elucidate the change in CuCl bulks during acetylene hydrochlorination, 5% CuCl + C was evaluated for acetylene hydrochlorination, and 5% CuCl + C samples used during different periods were characterized by technology such as inductively coupled plasma-optical emission spectrometry (ICP-OES), X-ray diffraction (XRD), and scanning transmission electron microscopy (STEM). Figure 2a illustrates that the catalytic activity of 5% CuCl + C increased initially and stabilized around 50 h; then, the catalyst in the over 75 h run began to lose its effectiveness slowly, exhibiting excellent stability. Figure 2b confirms that as the reaction progressed, the diffraction peaks of CuCl gradually disappeared, and no observable CuCl peak position was detected in the 5% CuCl + C-u-110 h catalyst. This directly indicates that CuCl was either dispersed or lost in the reaction atmosphere. Table 1 shows that the Cu content in the 5% CuCl + C and 5% CuCl + C-u-110 h catalysts was 5.41% (mass) and 5.15% (mass), respectively. The 5% CuCl + C-u-110 h catalyst displayed a copper recovery rate of 95.2%, implying that CuCl dispersion dominated the reaction rather than being lost. However, copper was gradually depleted during the acetylene hydrochlorination procedure.

Table 1. Content of Cu on different Cu-based Catalysts.

Catalyst	Cu (%)	Recovery (%)
5% CuCl + C	5.41	-
5% CuCl + C-u-20 h-180 °C ¹	5.25	97.0
5% CuCl + C-u-110 h-180 °C	5.15	95.2
5% CuCl + C-u-20 h-190 °C	5.11	94.6
5% CuCl + C-u-20 h-200 °C	4.98	92.2
5% CuCl + C-u-20 h-210 °C	4.75	87.8
5% CuCl/C	5.50	-
5% CuCl/C-u-20 h-200 °C	5.15	93.6
5% CuCl + C _D ²	5.25	-

¹ The used catalysts were named in terms of their catalytic components, reaction temperature, used time as well, and content of Cu, e.g., 5% CuCl + C-u-20 h-200 °C indicates the CuCl + C catalyst with a copper content of 5wt% used for 20 h under the 200 °C condition. ² 5% CuCl + C_D denotes 5% CuCl + C thermally treated at 350 °C for 3 h in a nitrogen atmosphere.

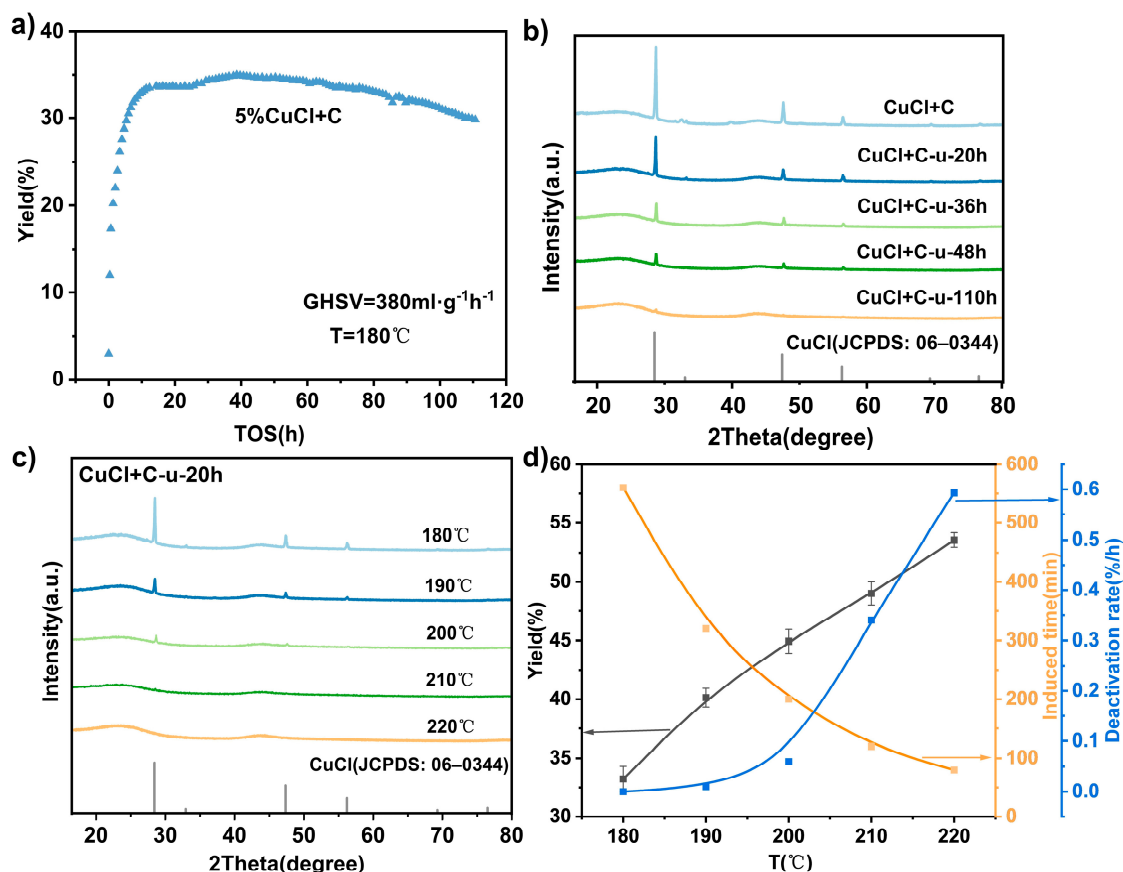


Figure 2. (a) The C_2H_3Cl yield of the 5% CuCl + C catalyst in 100 h. Test conditions: $GHSV(C_2H_2) = 380 \text{ mL}\cdot\text{h}^{-1}\cdot\text{g}^{-1}$, $V_{HCl}:V_{C_2H_2} = 1.1$, and $T = 180 \text{ }^\circ\text{C}$. (b) XRD patterns of CuCl + C used for different periods. (c) XRD of 5% CuCl + C used in the range of $180 \text{ }^\circ\text{C}$ to $220 \text{ }^\circ\text{C}$. (d) The catalytic performance of 5% CuCl + C catalysts with different temperatures. (Reaction conditions: temperature ranging from $180 \text{ }^\circ\text{C}$ to $220 \text{ }^\circ\text{C}$, $GHSV(C_2H_2) = 380 \text{ mL}\cdot\text{h}^{-1}\cdot\text{g}^{-1}$, and $V_{HCl}:V_{C_2H_2} = 1.1$). The deactivation rate in this figure refers to the average deactivation rate of the catalyst within 10 h of reaction from the highest active point. Error bars indicate the lowest and highest C_2H_3Cl yields obtained within three independent measurements. The induced period and deactivation rate represent the averages of the three replicates.

Similarly, Figure 3a illustrates micron-sized CuCl bulks affixed to the activated carbon surface of the fresh 5% CuCl + C catalyst. As shown in Figure 3b, CuCl + C-u-20 h still contained CuCl grains with dispersed nanoparticles throughout. To further analyze the dispersion of CuCl, HAADF-STEM images of 5% CuCl + C after testing for 48 h (5% CuCl + C-u-48 h) and 110 h (5% CuCl + C-u-110 h) are displayed in Figure 3c,d, respectively. As shown in Figure 3c, CuCl grains were not observed to aggregate, but a large number of homogeneously dispersed Cu nanoparticles around 2 nm in size and monodispersed copper were present on the activated carbon. Similarly, as shown in Figure 3d, there were mainly small Cu clusters and single atoms present in CuCl + C-u-110 h. The STEM analysis of 5% CuCl + C used for different periods demonstrates that the CuCl bulks underwent an extensive structural transformation into small clusters and single atoms during acetylene hydrochlorination, which is consistent with ICP-OES and XRD analyses. Meanwhile, during the reaction, the surface area of the catalyst decreased from $1047.11 \text{ m}^2/\text{g}$ of 5% CuCl + C to $611.6 \text{ m}^2/\text{g}$ of 5% CuCl + C-u-110 h, which might have been caused by the pore clogging and carbon deposition that occurred during the reaction-induced dispersion of CuCl on activated carbon, as indicated by the BET analysis presented in Table 2.

Table 2. Structure and texture parameters of the catalysts.

Catalyst	S_{Total} (m^2/g)	S_{Micro} (m^2/g)	V_{Micro} (cm^3/g)
5% CuCl + C	1047.11	1022.85	0.405
5% CuCl + C _D	995	936.8	0.366
5% CuCl/C	904.36	880.95	0.349
5% CuCl + C-u-20 h-180 °C *	905.5	875.8	0.345
5% CuCl + C-u-48 h-180 °C	724.7	664.8	0.261
5% CuCl + C-u-110 h-180 °C	611.6	569.8	0.226
5% CuCl + C-u-20 h-190 °C	883.4	834.6	0.326
5% CuCl + C-u-20 h-200 °C	855.9	799.9	0.313
5% CuCl + C-u-20 h-210 °C	701.66	672.15	0.270
1% CuCl + C-u-20 h-200 °C	1036	999.5	0.393
3% CuCl + C-u-20 h-200 °C	961.3	917.9	0.361
7% CuCl + C-u-20 h-200 °C	716.04	689.6	0.272
10% CuCl + C-u-20 h-200 °C	497.3	471.7	0.189
5% CuCl + C _D -u-20 h-200 °C	741.6	696.7	0.276
5% CuCl/C-u-20 h-200 °C	557.6	533.9	0.216

* The used catalysts were named in terms of their catalytic components, reaction temperature, used time, and content of Cu, e.g., 5% CuCl + C-u-20 h-200 °C indicates the CuCl + C catalyst with a copper content of 5wt% used for 20 h under the 200 °C condition.

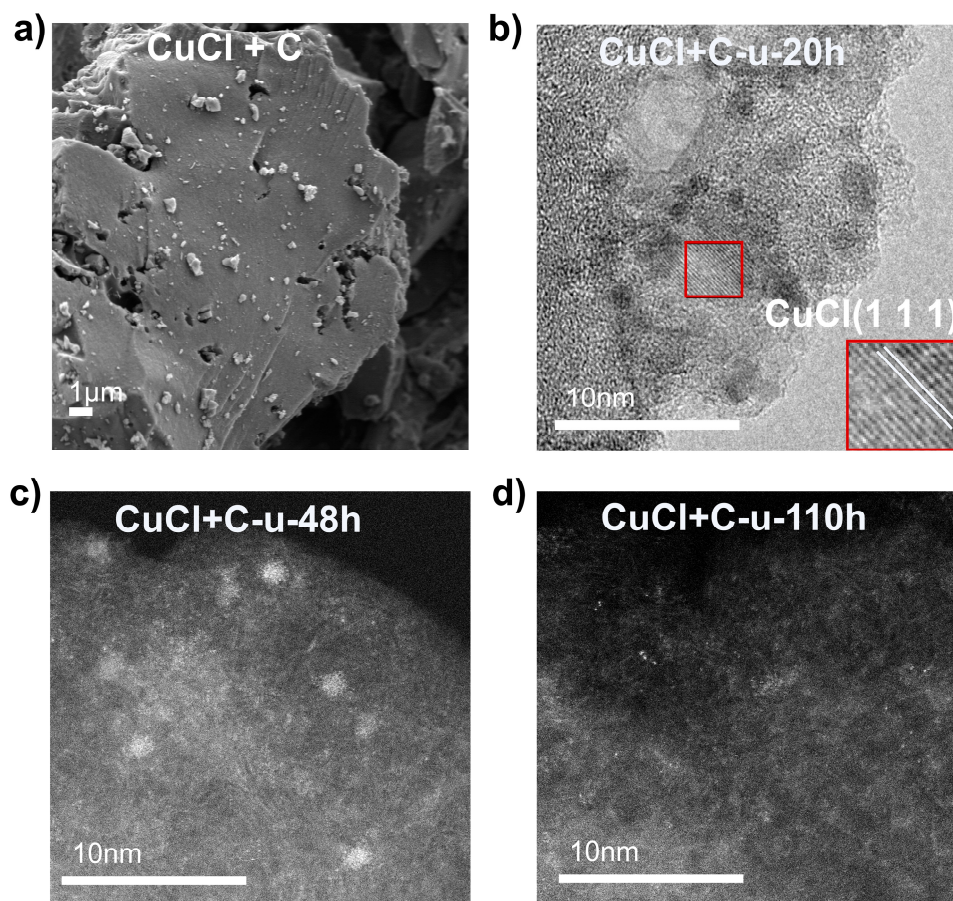


Figure 3. (a) SEM image of fresh CuCl + C catalysts. (b) TEM of CuCl + C used for 20 h. (c) HAADF-STEM of CuCl + C used for 48 h. (d) HAADF-STEM of CuCl + C used for 110 h.

2.3. The Effects of Temperature on the Performance of CuCl + C Catalysts

As illustrated in Figure 2d, the effects of temperature on the performance of CuCl + C catalysts were investigated with varying conditions of $T = 180\text{--}220\text{ °C}$, $C_2H_2\text{-GHSV} = 380\text{ mL}\cdot\text{h}^{-1}\cdot\text{g}^{-1}$, and $V_{\text{HCl}}/V_{\text{C}_2\text{H}_2} = 1.1$. The induction period was observed to decrease with increasing temperature, while the catalytic activity showed a positive correlation with

temperature. The diffraction peaks of CuCl in 5% CuCl + C catalysts used for 20 h also obviously decreased with higher temperatures, indicating an accelerated dispersion or migration of CuCl components over the surface of activated carbon. This can be attributed to the increased external energy provided by high temperatures, which caused atoms to break the constraint of lattice bonding easily and enhanced the reaction rate of acetylene hydrochlorination [31]. However, as shown in Figure 2d, the excellent catalytic performance of 5% CuCl + C at temperatures exceeding 200 °C was short-lived due to the accelerated deactivation of the catalyst, suggesting high temperature is not an optimal way to improve the catalytic performance of 5% CuCl + C catalysts. Table 1 also reveals that the Cu content of 5% CuCl + C used for 20 h with increasing reaction temperature decreased, while Table 2 shows a decline in the BET surface area and total pore volume of the catalyst at higher temperatures. These results suggest that high temperatures provided adequate energy, promoting the diffusion of CuCl and the loss of Cu through a reaction gas. Therefore, we have chosen a reaction temperature of 200 °C for our next exploration, which exhibited moderate activity and moderate deactivation rate.

2.4. Effect of the Amount and Dispersion of CuCl on CuCl + C Catalyst Performance

The prepared catalysts with different CuCl loadings were tested for the acetylene hydrochlorination reaction; the maximum yield during the test period (20 h) is illustrated in Figure 4a. At 200 °C, the yield of vinyl chloride initially increased before declining within the 1–10% loading range. The catalytic activities of catalysts over the 20 h run with increasing loading demonstrated a clear volcanic relationship with Cu loading. The optimal yield was achieved at the 5% loading level. Figure 4c reveals that increasing copper loading in the CuCl + C catalyst resulted in a rise in the residual CuCl crystal of CuCl + C, indicating that the dispersion of CuCl became increasingly difficult as the amount of CuCl increased. According to Table 2, high Cu loading led to significant reductions in the catalysts' surface area and pore volume. Particularly, the surface area of 10% CuCl + C decreased from 934.4 m²/g before the reaction to 497.3 m²/g after the reaction. Therefore, CuCl-induced pore clogging under high Cu loading conditions might have obstructed the mass and heat transfer of the reaction, resulting in reduced catalytic activity.

In addition, we conducted an investigation into how the dispersion of CuCl affected the activity and stability of the catalyst. By adjusting the degree of grinding and preheating time of the catalysts, we were able to obtain four different dispersions of 5% CuCl + C, with dispersion values (D) of 1, 0.89, 0.094, and 0. Figure 4b shows that the sample with $D = 1$ (i.e., 5% CuCl + C_D) did not show any diffraction peak of CuCl. As shown in Figure 5, copper mainly existed in the form of two-dimensional small clusters and single atoms in the 5% CuCl + C_D , indicating that CuCl was highly dispersed on activated carbon after thermal treatment. EDS data show that Cu and Cl elements were uniformly distributed on the activated carbon, which is consistent with the XRD and STEM results. As shown in Figure 4d, the dispersion of CuCl exhibited a linear relationship with catalyst activity and the deactivation rate. The initial catalytic activity of 5% CuCl + C and 5% CuCl + C_M obtained via the dry mixing method was low (37% and 34% C₂H₃Cl yield, respectively), despite their high stability. It is possible that the low activity of the two samples was due a number of unscattered CuCl bulks at the beginning of the reaction. On the other hand, 5% CuCl + C_D exhibited the highest yield, but this high yield was accompanied by a high level of deactivation, which was not observed in catalysts with low dispersions (5% CuCl + C and 5% CuCl + C_M) over the same testing period. In the initial stages of the reaction, the C₂H₃Cl yield of CuCl + C_D was high because CuCl was highly dispersed in fresh 5% CuCl + C; correspondingly, its deactivation rate was quick. This experiment confirmed that the dispersion of CuCl on activated carbon may be directly proportional to its catalytic activity and inversely proportional to its stability under our reaction condition. In other words, while greater CuCl dispersion resulted in increased activities, it corresponded with worse durability for acetylene hydrochlorination [32]. Although several CuCl bulks

presented in the fresh catalysts synthesized using the dry mixing method, they were induced to disperse during the reaction, resulting in good stability.

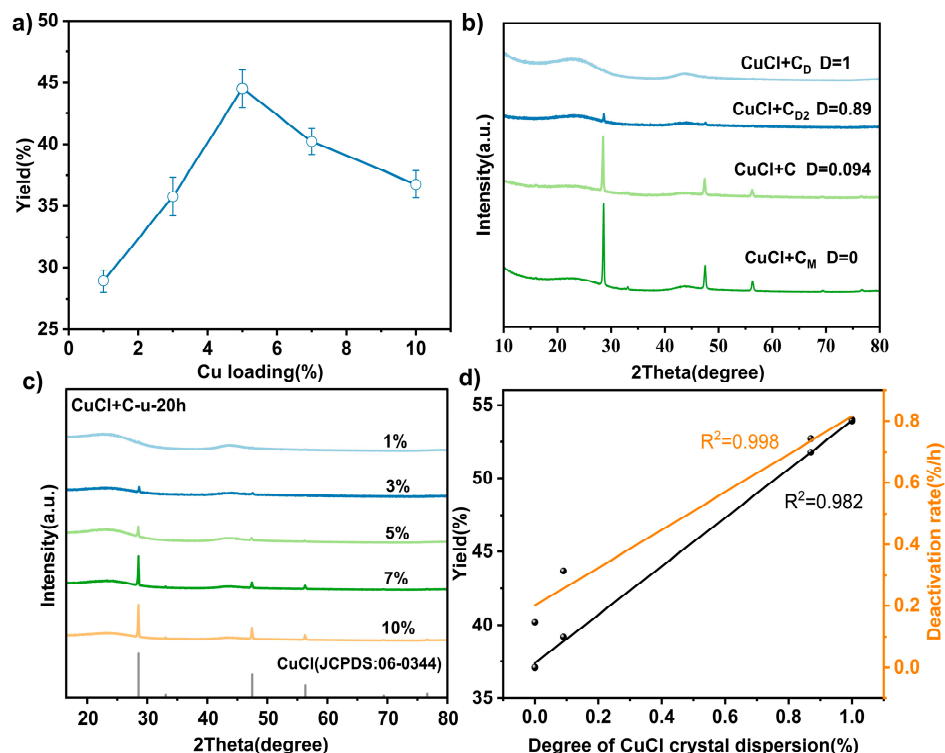


Figure 4. (a) C_2H_3Cl yield over $CuCl + C$ catalysts with different Cu loadings (reaction conditions: $200\text{ }^\circ C$, $GHSV(C_2H_2) = 380\text{ mL}\cdot h^{-1}\cdot g^{-1}$, and $V_{HCl}:V_{C_2H_2} = 1.1$). Error bars indicate the lowest and highest C_2H_3Cl yield obtained within three independent measurements. (b) XRD of catalysts with different $CuCl$ dispersions. (c) XRD of $CuCl + C$ with different Cu loadings used for 20 h. (d) C_2H_3Cl yield and average deactivation rate over 5% $CuCl + C$ catalysts with different $CuCl$ crystal dispersions.

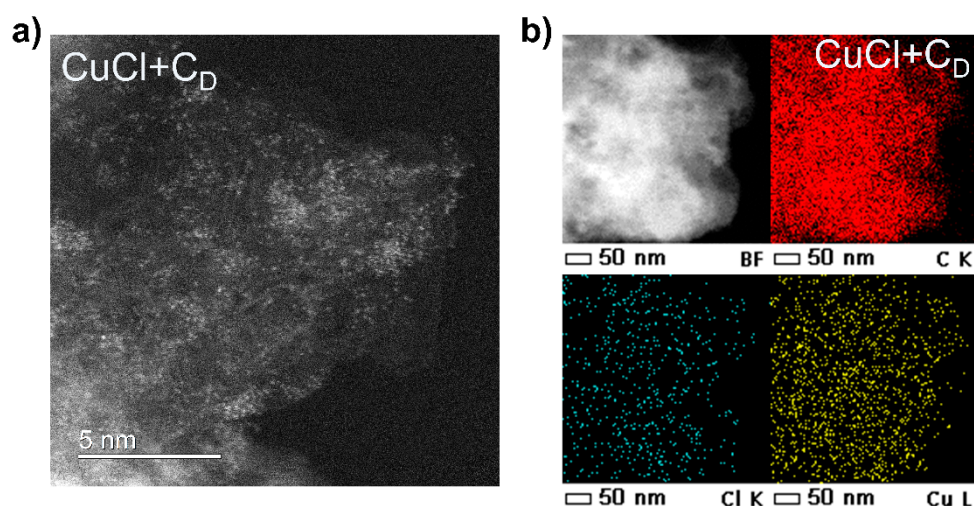


Figure 5. (a) HAADF-STEM of $CuCl + C_D$. (b) STEM-EDS of $CuCl + C_D$.

2.5. Comparison between Dry Mixing Method and Impregnation Method

In this experiment, we conducted a comparison of catalytic performance between 5% $CuCl + C$ synthesized by dry mixing, 5% $CuCl + C_D$ obtained by thermal dispersion, and 5% $CuCl/C$ prepared by impregnation. As depicted in Figure 6a, the C_2H_3Cl yield of 5% $CuCl + C_D$ decreased from 54.3% to 43.2%, while the C_2H_3Cl yield of 5% $CuCl/C$

decreased from 48.3% to 37%. This suggested that the catalytic activity of 5% CuCl + C_D was high compared to that of 5% CuCl/C, but the two exhibited similar stability with a 0.8%/h deactivation rate. Interestingly, the initial activity of 5% CuCl + C was lower than that of 5% CuCl/C, but it surpassed that of 5% CuCl/C after 5 h of reaction due to its superior durability. After 15 h, the yield of 5% CuCl + C reached 45%, far exceeding that of 5% CuCl/C. Therefore, the 5% CuCl + C obtained by the dry mixing method showed the highest catalytic stability among the three catalysts. A detailed analysis of the three catalysts was conducted, as shown in Figure 6. The XPS spectra (Figure S3) reveal that the copper state in the three catalysts mainly existed as Cu²⁺ species with 934.4 eV bonding energy [11]. However, since XPS is a surface analysis technique and owing to the oxophilicity of copper, the XPS analysis may deviate significantly from the actual situation. To increase the credibility of the data, we also conducted H₂-TPR characterization, where the peak area represents the H₂ consumption of the catalysts, and the reduction temperature represents the difficulty of copper reduction. As seen in Figure 6b, the 5% CuCl + C catalyst exhibits three reduction peaks at 350 °C, 380 °C, and 600 °C, corresponding to Cu²⁺ reduction, Cu⁺ reduction, and activated carbon reduction, respectively. These three reduction peaks can also be observed on the 5% CuCl/C and 5% CuCl + C_D catalysts. Additionally, given that the precursors of all three catalysts are CuCl, we can observe that the hydrogen consumption of 5% CuCl + C and 5% CuCl + C_D was significantly lower than that of 5% CuCl/C, indicating that 5% CuCl/C underwent extensive oxidation during preparation, with the valence state of copper increasing. The peak areas (see Figure S3) of the three catalysts used for 20 h were comparable and slightly reduced compared to pre-reaction levels, suggesting that 5% CuCl/C underwent greater reduction than 5% CuCl + C and 5% CuCl + C_D during the reaction. In addition, to comprehend the valence transition of copper in the reaction, 5% CuCl₂ + C was evaluated for acetylene hydrochlorination. As shown in Figure S4, the diffraction peak of CuCl₂ was clearly visible in the fresh 5% CuCl₂ + C catalyst; however, the CuCl₂ was completely replaced by the generation of CuCl crystals when the 5% CuCl₂ + C catalyst was used for over 1 h. The reported phenomenon show that CuCl₂ crystals were quickly reduced to CuCl crystals in the atmosphere of acetylene hydrochlorination; subsequently, the CuCl crystals were slowly dispersed and consumed. Thus, it can be inferred that high-valence copper ions are highly unstable in this atmosphere, and monodispersed CuCl is the real active site for acetylene hydrochlorination, as found in previous studies [11]. Furthermore, the samples were analyzed using TPD characterization to study their reactant adsorption. The desorption temperature indicates adsorption strength, and the area under the desorption peak represents the amount of adsorption. As shown in Figure 6c, the overall desorption peak area of acetylene was nearly identical for 5% CuCl/C and 5% CuCl + C. However, 5% CuCl/C exhibited two desorption peaks at 150 °C and 350 °C, while 5% CuCl + C mainly adsorbed chemically, as indicated by the primary desorption temperature occurring at 350 °C.

Thermal gravity analysis conducted under oxidizing conditions was used to obtain information regarding carbonaceous material deposition on catalysts. As shown in Figure 6d,e, coke deposition of 5% CuCl + C was found to be negligible over the 20 h run at 200 °C, which evidently decreased compared to 5% CuCl/C. The BET surface areas of 5% CuCl + C, 5% CuCl + C_D, and 5% CuCl/C were 1047.11 m²/g, 995 m²/g, and 904.6 m²/g, respectively. After the reaction, the BET surface areas of the three catalysts were 855.9 m²/g, 741.6 m²/g, and 557.6 m²/g. 5% CuCl + C and 5% CuCl + C_D prepared by the dry mixing method reduced the surface area loss compared with 5% CuCl/C. Thus, different methods of synthesis result in different surface properties, often leading to a difference in catalytic performance [33]. Based on the above results, it can be concluded that the catalytic performance of 5% CuCl + C and 5% CuCl + C_D was superior to that of 5% CuCl/C prepared by the ordinary impregnation method. The dry mixing method offered the advantage of maximally preserving the porous structure of activated carbon and active sites. Lastly, 5% CuCl + C was evaluated under industrially relevant catalytic conditions for non-precious metals for 100 h (GHSV (C₂H₂) = 60 mL·h⁻¹·g⁻¹, V_{HCl}:V_{C₂H₂} = 1.1, and T = 200 °C). As

shown in Figure 6f, the initial activity of 5% CuCl + C was 93.3%, which was maintained at 92.9% after 100 h long-term testing, with a deactivation rate of $0.004\% \text{ h}^{-1}$. It also exhibited remarkable stability, with a low activity decay ($0.004\% \text{ h}^{-1}$) approximately 100 times lower than state-of-the-art precious metal catalysts [11]. In addition, the dry mixing method without the introduction of other heteroatoms and solvents was simple, cost-effective, and environmentally friendly. Thus, the dry mixing method is an environmentally responsible choice for preparing copper-based catalysts to be reaction-induced into a CuCl single site for acetylene hydrochlorination.

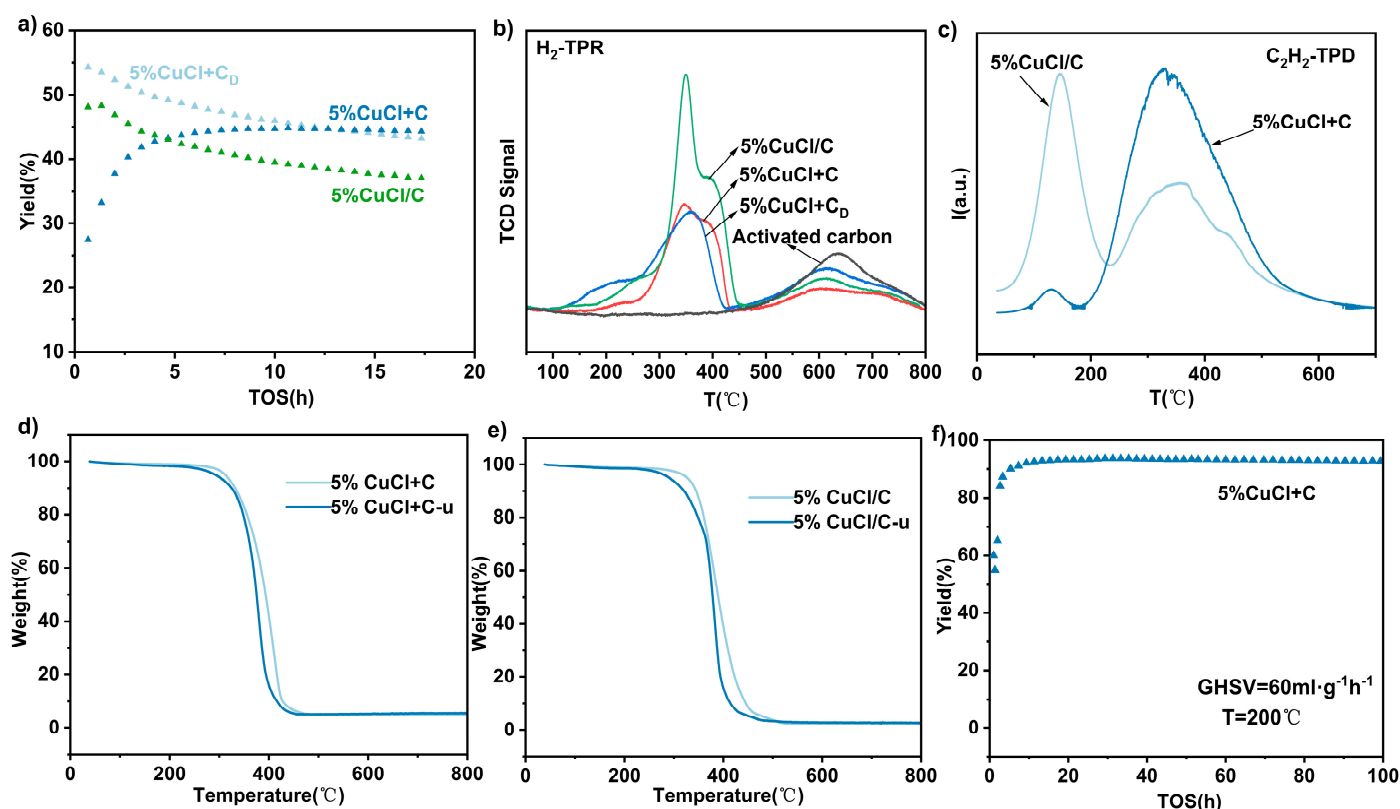


Figure 6. (a) $\text{C}_2\text{H}_3\text{Cl}$ yield over the three catalysts. (b) H_2 -TPR of the three catalysts. (c) C_2H_2 -TPD of different samples. (d) TG of fresh and used CuCl + C. (e) TG of fresh and used CuCl/C. (f) $\text{C}_2\text{H}_3\text{Cl}$ yield of 5% CuCl + C. Test conditions: $\text{GHSV}(\text{C}_2\text{H}_2) = 60 \text{ mL}\cdot\text{h}^{-1}\cdot\text{g}^{-1}$, $V_{\text{HCl}}:V_{\text{C}_2\text{H}_2} = 1.1$, and $T = 200 \text{ }^\circ\text{C}$.

3. Materials and Methods

3.1. Materials

The following materials were used: cuprous chloride (98%, Innochem, Beijing, China), cuprous bromide (99.5%, Innochem, Beijing, China), cuprous iodide (99.5%, Innochem, Beijing, China), nitric acid (AR, 68%, Damao, Tianjin, China), hydrochloric acid (AR, 34–46%, Damao, Tianjin, China), activated carbon (neutral, coconut carbon, 80–160 mesh, China), HCl (gas, 99%, Date, Dalian, China), and C_2H_2 (gas, 98%, Date, Dalian, China).

3.2. Catalyst Preparation

Activated carbon (80–160 mesh) was purified by stirring in an aqueous nitric acid solution for 30 min, followed by thorough washing with deionized water and drying at 473 K for 12 h.

5% CuCl + C was prepared via a dry mixing method by mixing and grinding 0.236 g CuCl corresponding to a nominal content of 5wt% with 2.76 g pretreated activated carbon. Specifically, the CuCl salt was ground for 20 min and passed through a 160-mesh sieve. The resulting CuCl was then mixed with the dried activated carbon to obtain 5% CuCl + C. This standard procedure was adapted to obtain $\text{CuX} + \text{C}$ ($X = \text{Cl}, \text{Br}, \text{I}$) by replacing

CuCl with the appropriate amount of CuBr, CuI, or CuCl₂. For reference purposes, catalysts with different nominal Cu contents (1, 3, 7, and 10wt%) were prepared, following the same procedure for CuCl + C.

At the same time, 5% CuCl + C_M was prepared by taking the same mass of CuCl salts and only mixing them directly with activated carbon, without grinding. Subsequently, two pieces of 5% CuCl + C were thermally treated at 350 °C for 3 h and 30 min in a nitrogen atmosphere, denoted as 5% CuCl + C_D and 5% CuCl + C_{D2}, respectively, and the above three catalysts, together with 5% CuCl + C, constituted a series of dry-mixing catalysts with different degrees of dispersion. The CuCl dispersion was determined by measuring the peak area at $2\theta = 28.5^\circ$ in the XRD spectrum. The peak areas at $2\theta = 28.5^\circ$ are expressed as S_M, S, S_D, and S_{D2}, which correspond to the 5% CuCl + C_M, 5% CuCl + C, 5% CuCl + C_D, and 5% CuCl + C_{D2} catalysts, respectively. The dispersion (D) of 5% CuCl + C catalyst was calculated based on Equation (1) as follows:

$$\text{Dispersion (D)} = 1 - S/S_M. \quad (1)$$

As a reference, 5% CuCl/C was prepared via an incipient wetness impregnation method [3,7,34]. An amount of 0.236 g of CuCl precursor was dissolved in 3 mL hydrochloric acid. After stirring for 20 min, the solution was added dropwise to the pretreated-activated carbon. The obtained system was aged at 298 K for 2 h and finally dried at 473 K for 12 h to obtain 5wt% CuCl/C. In order to make the discussion clear, the used catalysts were named in terms of their catalytic components, reaction temperature, used time, and content of Cu, e.g., 5% CuCl + C-u-20 h-200 °C indicates the CuCl + C catalyst with a copper content of 5wt% used for 20 h under the 200 °C condition.

3.3. Catalyst Characterization

X-ray diffraction (XRD) measurements were performed using an Empyrean X-ray diffractometer (Malvern Panalytical, Shanghai, China) with monochromatized Cu K α radiation ($\lambda = 1.5406 \text{ \AA}$) operating in the 2θ scan range from 10° to 90°. Temperature-programmed reduction (TPR) experiments were performed using an AutoChem II-DSMS (Micromeritics, Norcross, GA, USA) instrument in a micro-flow reactor fed with a 5% H₂/Ar mixture at a flow rate of 20 mL/min. The temperature was increased from 30 to 800 °C at a heating rate of 10 °C·min⁻¹. X-ray photoelectron spectroscopy (XPS) spectra were recorded using an ESCALAB 250Xi spectroscope (Thermo Fisher, Waltham, MA, USA). The binding energy was calibrated concerning the C 1s level of contaminated carbon at 284.80 eV. Brunauer–Emmett–Teller (BET) specified surface area analysis was conducted using a Quantachrome Quadrasorb evo instrument. High-angle annular dark-field scanning transmission electron microscopy (HAADF-STEM) imaging modes were implemented in an aberration-corrected JEOL ARM200CF microscope (JEOL Ltd., Tokyo, Japan) operating at 200 kV. TEM was carried out using a JEM-2100 electron microscope. Inductively coupled plasma–optical emission spectrometry (ICP-OES) was measured to determine the loading of Cu for the catalysts with a 7300DV instrument (Varian, Palo Alto, CA, USA). Thermal gravity analysis (TG-DTG) analysis was conducted with an STA449F5-Thermostar (Netzsch, Shanghai, China) in air. The temperature was increased from 30 to 800 °C at a heating rate of 10 °C·min⁻¹. Temperature-programmed desorption (TPD) analysis of the samples was performed with an AutoChem II-OmniStar (Micromeritics, Norcross, GA, USA). The temperature was increased from 50 to 700 °C at a heating rate of 10 °C·min⁻¹.

3.4. Catalyst Tests

Acetylene hydrochlorination was studied at atmospheric pressure in a continuous-flow, fixed-bed microreactor ($\Phi 12 \text{ mm} \times 460 \text{ mm}$) as reported elsewhere [3,7,11,16]. The temperature was controlled by a thermocouple located in a quartz thermowell with the tip positioned in the center of the catalyst bed. First, a 1.9 g catalyst was loaded in the reactor, followed by sweeping with nitrogen (N₂) gas at 473 K for at least 0.5 h to remove impurities

like water and air. Subsequently, C_2H_2 (12 mL/min) and HCl (13.2 mL/min) were fed through filters with an acetylene gas hourly space velocity (GHSV) of $380 \text{ mL}\cdot\text{h}^{-1}\cdot\text{g}^{-1}$ at 473 K. The effluent gas was passed into the NaOH solution and drier, followed by analysis using a mass spectrometer (Agilent, GC 8860, Shanghai, China). After the tests, the reactor was quenched to room temperature in N_2 flow, and the catalytic materials were retrieved for further characterization. As VCM was the only product tested, the catalytic activity is presented as the yield of VCM (Y), calculated according to Equation (2), where S_{VCM} and S_A represents the molar flows of VCM and C_2H_2 , respectively, at the reactor outlet and inlet [11]. The experimental error in VCM yield was $\pm 1\%$ for repeated tests.

$$Y_{VCM} = \frac{S_{VCM}}{S_A} \times 100\% \quad (2)$$

The catalyst deactivation rate (D) was calculated according to Equation (3), where $Y_{Highest}$ represents the highest VCM yield over the reaction time, and Y_{10H} represents the yield after 10 h of reaction from the highest point with reference to the average deactivation rate of the catalyst within 10 h of reaction from the highest active point.

$$D = (Y_{Highest} - Y_{10H}) / 10 \text{ h} \quad (3)$$

4. Conclusions

Herein, we presented a dry mixing method to synthesize copper-based catalysts to be reaction-induced to form a copper single site for acetylene hydrochlorination. Under the same conditions, the 5% CuCl + C catalyst prepared by the dry mixing method exhibited higher stability than the 5% CuCl/C catalyst obtained through the conventional impregnation method. The C_2H_3Cl yield of 5% CuCl + C decreased from 93.7% to 92.9% after 100 h of reaction under the condition of $GHSV(C_2H_2) = 60 \text{ mL}\cdot\text{h}^{-1}\cdot\text{g}^{-1}$. This dry mixing method allowed for the facile preparation of copper-based catalysts without solvents, in addition to effectively preserving the active copper species and porous structure of activated carbon, representing a new strategy for the preparation of single-site catalysts for acetylene hydrochlorination.

Supplementary Materials: The following supporting information can be downloaded at: <https://www.mdpi.com/article/10.3390/catal14030207/s1>, Figure S1: SEM image of different samples; Figure S2: XPS of 5% CuCl + C, 5% CuCl + C_D , and 5% CuCl/C; Figure S3: H_2 -TPR of 5% CuCl + C-u, 5% CuCl + C_D -u, and 5% CuCl/C-u; Figure S4: (a) The catalytic performance of $CuCl_2 + C$; (b) The XRD of 5% $CuCl_2 + C$.

Author Contributions: Conceptualization, Y.F.; methodology, Y.F.; software, Y.F. and J.Z.; validation, Y.F. and J.Z.; formal analysis, Y.F.; investigation, Y.F.; resources, J.H.; data curation, Y.F.; writing—original draft preparation, Y.F.; writing—review and editing, J.H. and X.S.; visualization, J.Z.; supervision, X.S. and J.H.; project administration, X.S. and J.H.; funding acquisition, J.H. All authors have read and agreed to the published version of the manuscript.

Funding: This work was financially supported by the “Strategic Priority Research Program” of the Chinese Academy of Sciences (XDA21030900).

Data Availability Statement: The data presented in this study are available upon request from the corresponding author. The data are not publicly available due to privacy or ethical restrictions.

Conflicts of Interest: The authors declare no conflicts of interest.

References

1. Liu, L.; Corma, A. Metal Catalysts for Heterogeneous Catalysis: From Single Atoms to Nanoclusters and Nanoparticles. *Chem. Rev.* **2018**, *118*, 4981–5079. [[CrossRef](#)] [[PubMed](#)]
2. Corma, A. Heterogeneous Catalysis: Understanding for Designing, and Designing for Applications. *Angew. Chem. Int. Ed.* **2016**, *55*, 6112–6113. [[CrossRef](#)]

3. Sun, X.; Dawson, S.R.; Parmentier, T.E.; Malta, G.; Davies, T.E.; He, Q.; Lu, L.; Morgan, D.J.; Carthey, N.; Johnston, P.; et al. Facile Synthesis of Precious-Metal Single-Site Catalysts Using Organic Solvents. *Nat. Chem.* **2020**, *12*, 560–567. [[CrossRef](#)] [[PubMed](#)]
4. Kaiser, S.K.; Chen, Z.; Faust Akl, D.; Mitchell, S.; Pérez-Ramírez, J. Single-Atom Catalysts across the Periodic Table. *Chem. Rev.* **2020**, *120*, 11703–11809. [[CrossRef](#)]
5. Malta, G.; Freakley, S.J.; Kondrat, S.A.; Hutchings, G.J. Acetylene Hydrochlorination Using Au/Carbon: A Journey towards Single Site Catalysis. *Chem. Commun.* **2017**, *53*, 11733–11746. [[CrossRef](#)]
6. Johnston, P.; Carthey, N.; Hutchings, G.J. Discovery, Development, and Commercialization of Gold Catalysts for Acetylene Hydrochlorination. *J. Am. Chem. Soc.* **2015**, *137*, 14548–14557. [[CrossRef](#)] [[PubMed](#)]
7. Malta, G.; Kondrat, S.A.; Freakley, S.J.; Davies, C.J.; Lu, L.; Dawson, S.; Thetford, A.; Gibson, E.K.; Morgan, D.J.; Jones, W.; et al. Identification of Single-Site Gold Catalysis in Acetylene Hydrochlorination. *Science* **2017**, *355*, 1399–1403. [[CrossRef](#)] [[PubMed](#)]
8. Lin, R.; Amrute, A.P.; Pérez-Ramírez, J. Halogen-Mediated Conversion of Hydrocarbons to Commodities. *Chem. Rev.* **2017**, *117*, 4182–4247. [[CrossRef](#)]
9. Ciacci, L.; Passarini, F.; Vassura, I. The European PVC Cycle: In-Use Stock and Flows. *Resour. Conserv. Recycl.* **2017**, *123*, 108–116. [[CrossRef](#)]
10. Trotsuş, I.-T.; Zimmermann, T.; Schüth, F. Catalytic Reactions of Acetylene: A Feedstock for the Chemical Industry Revisited. *Chem. Rev.* **2014**, *114*, 1761–1782. [[CrossRef](#)]
11. Faust Akl, D.; Giannakakis, G.; Ruiz-Ferrando, A.; Agrachev, M.; Medrano-García, J.D.; Guillén-Gosálbez, G.; Jeschke, G.; Clark, A.H.; Safonova, O.V.; Mitchell, S.; et al. Reaction-Induced Formation of Stable Mononuclear Cu(I)Cl Species on Carbon for Low-Footprint Vinyl Chloride Production. *Adv. Mater.* **2023**, *35*, 2211464. [[CrossRef](#)]
12. Zhu, M.; Wang, Q.; Chen, K.; Wang, Y.; Huang, C.; Dai, H.; Yu, F.; Kang, L.; Dai, B. Development of a Heterogeneous Non-Mercury Catalyst for Acetylene Hydrochlorination. *ACS Catal.* **2015**, *5*, 5306–5316. [[CrossRef](#)]
13. Kaiser, S.K.; Lin, R.; Mitchell, S.; Fako, E.; Krumeich, F.; Hauert, R.; Safonova, O.V.; Kondratenko, V.A.; Kondratenko, E.V.; Collins, S.M.; et al. Controlling the Speciation and Reactivity of Carbon-Supported Gold Nanostructures for Catalysed Acetylene Hydrochlorination. *Chem. Sci.* **2019**, *10*, 359–369. [[CrossRef](#)] [[PubMed](#)]
14. Hutchings, G. Vapor Phase Hydrochlorination of Acetylene: Correlation of Catalytic Activity of Supported Metal Chloride Catalysts. *J. Catal.* **1985**, *96*, 292–295. [[CrossRef](#)]
15. Ye, L.; Duan, X.; Wu, S.; Wu, T.-S.; Zhao, Y.; Robertson, A.W.; Chou, H.-L.; Zheng, J.; Ayvalı, T.; Day, S.; et al. Self-Regeneration of Au/CeO₂ Based Catalysts with Enhanced Activity and Ultra-Stability for Acetylene Hydrochlorination. *Nat. Commun.* **2019**, *10*, 914. [[CrossRef](#)]
16. Kaiser, S.K.; Fako, E.; Surin, I.; Krumeich, F.; Kondratenko, V.A.; Kondratenko, E.V.; Clark, A.H.; López, N.; Pérez-Ramírez, J. Performance Descriptors of Nanostructured Metal Catalysts for Acetylene Hydrochlorination. *Nat. Nanotechnol.* **2022**, *17*, 606–612. [[CrossRef](#)]
17. Kaiser, S.K.; Fako, E.; Manzocchi, G.; Krumeich, F.; Hauert, R.; Clark, A.H.; Safonova, O.V.; López, N.; Pérez-Ramírez, J. Nanostructuring Unlocks High Performance of Platinum Single-Atom Catalysts for Stable Vinyl Chloride Production. *Nat. Catal.* **2020**, *3*, 376–385. [[CrossRef](#)]
18. Pu, Y.; Zhang, J.; Yu, L.; Jin, Y.; Li, W. Active Ruthenium Species in Acetylene Hydrochlorination. *Appl. Catal. A Gen.* **2014**, *488*, 28–36. [[CrossRef](#)]
19. Zhang, J.; Sheng, W.; Guo, C.; Li, W. Acetylene Hydrochlorination over Bimetallic Ru-Based Catalysts. *RSC Adv.* **2013**, *3*, 21062–21068. [[CrossRef](#)]
20. Xu, J.; Zhao, J.; Zhang, T.; Di, X.; Gu, S.; Ni, J.; Li, X. Ultra-Low Ru-Promoted CuCl₂ as Highly Active Catalyst for the Hydrochlorination of Acetylene. *RSC Adv.* **2015**, *5*, 38159–38163. [[CrossRef](#)]
21. Fan, Y.; Xu, H.; Liu, Z.; Sun, S.; Huang, W.; Qu, Z.; Yan, N. Tunable Redox Cycle and Enhanced π -Complexation in Acetylene Hydrochlorination over RuCu Catalysts. *ACS Catal.* **2022**, *12*, 7579–7588. [[CrossRef](#)]
22. Zhou, K.; Si, J.; Jia, J.; Huang, J.; Zhou, J.; Luo, G.; Wei, F. Reactivity Enhancement of N-CNTs in Green Catalysis of C₂H₂ Hydrochlorination by a Cu Catalyst. *RSC Adv.* **2014**, *4*, 7766–7769. [[CrossRef](#)]
23. Wang, B.; Zhang, T.; Liu, Y.; Li, W.; Zhang, H.; Zhang, J. Phosphine-Oxide Organic Ligand Improved Cu-Based Catalyst for Acetylene Hydrochlorination. *Appl. Catal. A Gen.* **2022**, *630*, 118461. [[CrossRef](#)]
24. Li, F.; Wang, X.; Zhang, P.; Wang, Q.; Zhu, M.; Dai, B. Nitrogen and Phosphorus Co-Doped Activated Carbon Induces High Density Cu⁺ Active Center for Acetylene Hydrochlorination. *Chin. J. Chem. Eng.* **2023**, *59*, 193–199. [[CrossRef](#)]
25. Wang, Y.; Nian, Y.; Zhang, J.; Li, W.; Han, Y. MOMTPPC Improved Cu-Based Heterogeneous Catalyst with High Efficiency for Acetylene Hydrochlorination. *Mol. Catal.* **2019**, *479*, 110612. [[CrossRef](#)]
26. Zhao, W.; Zhu, M.; Dai, B. The Preparation of Cu-g-C₃N₄/AC Catalyst for Acetylene Hydrochlorination. *Catalysts* **2016**, *6*, 193. [[CrossRef](#)]
27. Zhai, Y.; Zhao, J.; Di, X.; Di, S.; Wang, B.; Yue, Y.; Sheng, G.; Lai, H.; Guo, L.; Wang, H.; et al. Carbon-Supported Perovskite-like CsCuCl₃ Nanoparticles: A Highly Active and Cost-Effective Heterogeneous Catalyst for the Hydrochlorination of Acetylene to Vinyl Chloride. *Catal. Sci. Technol.* **2018**, *8*, 2901–2908. [[CrossRef](#)]
28. Wang, B.; Jin, C.; Shao, S.; Yue, Y.; Zhang, Y.; Wang, S.; Chang, R.; Zhang, H.; Zhao, J.; Li, X. Electron-Deficient Cu Site Catalyzed Acetylene Hydrochlorination. *Green Energy Environ.* **2023**, *8*, 1128–1140. [[CrossRef](#)]

29. Xie, Y.-C.; Tang, Y.-Q. Spontaneous Monolayer Dispersion of Oxides and Salts onto Surfaces of Supports: Applications to Heterogeneous Catalysis. In *Advances in Catalysis*; Elsevier: Amsterdam, The Netherlands, 1990; Volume 37, pp. 1–43, ISBN 978-0-12-007837-0.
30. Xiao, F.-S.; Zheng, S.; Sun, J.; Yu, R.; Qiu, S.; Xu, R. Dispersion of Inorganic Salts into Zeolites and Their Pore Modification. *J. Catal.* **1998**, *176*, 474–487. [[CrossRef](#)]
31. Wang, C.-B.; Cai, Y.; Wachs, I.E. Reaction-Induced Spreading of Metal Oxides onto Surfaces of Oxide Supports during Alcohol Oxidation: Phenomenon, Nature, and Mechanisms. *Langmuir* **1999**, *15*, 1223–1235. [[CrossRef](#)]
32. Morgan, K.; Goguet, A.; Hardacre, C. Metal Redispersion Strategies for Recycling of Supported Metal Catalysts: A Perspective. *ACS Catal.* **2015**, *5*, 3430–3445. [[CrossRef](#)]
33. Bennett, E.; Wilson, T.; Murphy, P.J.; Refson, K.; Hannon, A.C.; Imberti, S.; Callear, S.K.; Chass, G.A.; Parker, S.F. How the Surface Structure Determines the Properties of CuH. *Inorg. Chem.* **2015**, *54*, 2213–2220. [[CrossRef](#)] [[PubMed](#)]
34. Malta, G.; Kondrat, S.A.; Freakley, S.J.; Morgan, D.J.; Gibson, E.K.; Wells, P.P.; Aramini, M.; Gianolio, D.; Thompson, P.B.J.; Johnston, P.; et al. In Situ K-Edge X-ray Absorption Spectroscopy of the Ligand Environment of Single-Site Au/C Catalysts during Acetylene Hydrochlorination. *Chem. Sci.* **2020**, *11*, 7040–7052. [[CrossRef](#)] [[PubMed](#)]

Disclaimer/Publisher’s Note: The statements, opinions and data contained in all publications are solely those of the individual author(s) and contributor(s) and not of MDPI and/or the editor(s). MDPI and/or the editor(s) disclaim responsibility for any injury to people or property resulting from any ideas, methods, instructions or products referred to in the content.